

Dependence of Clustering on Galaxy Color for the Volume-limited Main Galaxy Sample of the SDSS6

XIN-FA DENG, JI-ZHOU HE, PING HU, AND XIN-SHENG MA

School of Science, Nanchang University, Jiangxi, 330031, China

Received 2008 August 14; accepted 2009 February 5; published 2009 March 12

ABSTRACT. From the volume-limited main galaxy sample of the Sloan Digital Sky Survey Data Release 6 (SDSS DR6), we construct three galaxy samples with different $g-r$ colors and perform comparative studies of clustering properties among them. It is found that the redder galaxies preferentially inhabit the dense groups and clusters.

1. INTRODUCTION

Many studies have shown that galaxies with different physical properties cluster differently (Brown et al. 2000; Carlberg et al. 2001; Norberg et al. 2001, 2002; Zehavi et al. 2002; Budavari et al. 2003; Madgwick et al. 2003; Hogg et al. 2003; Zehavi et al. 2005). In the past, a correlation function was the most popular method for investigating this issue. Brown et al. (2000) found that the galaxy correlation function depends strongly on color, with red galaxies more strongly clustered than blue galaxies by a factor of ≥ 5 at small scales, and that the slope of the correlation function varies with color, with $\gamma \approx 1.8$ for red galaxies and $\gamma \approx 1.5$ for blue galaxies. Due to the type dependence of clustering properties—late-type galaxies have considerably weaker clustering than early-type galaxies (Davis & Geller 1976; Loveday et al. 1995)—such behavior is consistent with color being correlated with morphological type. The study of Brown et al. (2000) also suggested that galaxy clustering is more strongly correlated with color than morphology. Using SDSS data, Zehavi et al. (2005) reached similar conclusions.

In using correlation functions, however, we cannot clearly understand the geometry of the distribution of galaxies. Maybe we should try some new methods to obtain more information about the color dependence of clustering properties. Some works have studied how the filaments depend on galaxy properties (Pandey & Bharadwaj 2006, 2007, 2008). Pandey & Bharadwaj (2006) showed that the blue galaxies and the spirals have a higher filamentarity as compared to the red galaxies and the ellipticals, respectively, at large filling factors. Pandey & Bharadwaj (2008) also found that star-forming (SF) galaxies, which are predominantly blue, have a more filamentary distribution than other galaxies, which are predominantly red. In this study, we intend to investigate the color dependence of clustering properties using a cluster analysis (Einasto et al. 1984) that is sensitive to the geometry of the distribution of galaxies. By this method, the galaxy sample can be separated into isolated

galaxies, close double and multiple galaxies, galaxy groups or clusters, and even superclusters that consist of clusters and strings of galaxies. Galaxy strings form bridges between superclusters and join all superclusters to a single infinite network. Our paper is organized as follows. In § 2, we describe the data used. The cluster analysis is discussed in § 3. In § 4, we investigate the color dependence of clustering properties. Our main results and conclusions are summarized in § 5.

2. DATA

Many survey properties of the SDSS were discussed in detail in the Early Data Release paper (Stoughton et al. 2002). Galaxy spectroscopic targets were selected by two algorithms. The main galaxy sample (Strauss et al. 2002) comprises galaxies brighter than $r_{\text{petro}} < 17.77$ (r -band apparent Petrosian magnitude). In our work, the data were downloaded from the Catalog Archive Server of SDSS Data Release 6 (Adelman-McCarthy et al. 2008) by the SDSS SQL Search (with SDSS flag: `bestPrimtarget & 64 > 0`) with high-confidence redshifts ($Z_{\text{warning}} \neq 16$, $Z_{\text{status}} \neq 0, 1$, and redshift confidence level $z_{\text{conf}} > 0.95$).¹ From this sample, we select 469,199 main galaxies in the redshift region $0.02 \leq z \leq 0.2$. We used the volume-limited main galaxy sample constructed by Deng et al. (2007), which contains 112,889 galaxies, extends to $Z_{\text{max}} = 0.089$, and is limited to the absolute magnitude region $-22.40 \leq M_r \leq -20.16$. The absolute magnitude M_r is calculated from the r -band apparent Petrosian magnitude using a polynomial fit formula (Park et al. 2005) for the mean K -correction within $0 < z < 0.3$:

$$K(z) = 2.3537(z - 0.1)^2 + 1.04423(z - 0.1) - 2.5 \log(1 + 0.1).$$

¹ For more information, see <http://www.sdss.org/dr6/>.

From this volume-limited sample, we construct three samples with $g-r$ color bins $0.4 \leq g-r < 0.6$, $0.6 \leq g-r < 0.8$, $0.8 \leq g-r < 1.0$, labeled S1–S3. S1 contains 19,752 galaxies, S2 includes 31,995 galaxies, and S3 has 55,743 galaxies.

In calculating the distance, we used a cosmological model with a matter density $\Omega_0 = 0.3$, cosmological constant $\Omega_A = 0.7$, and Hubble constant $H_0 = 100 h \text{ km s}^{-1} \text{ Mpc}^{-1}$ with $h = 0.7$.

3. CLUSTER ANALYSIS

The cluster analysis (Einasto et al. 1984) used here is actually the friends-of-friends algorithm by which the galaxy sample can be separated into individual systems at a given neighborhood radius R . Starting from one galaxy of the sample, we search all galaxies within a sphere of radius R around it and call these close galaxies “friends.” These friends and the starting galaxy are considered to belong to the same system. Around new neighbors, we continue the above procedure using the rule “any friend of my friend is my friend.” When no more new neighbors or friends can be added, then the procedure stops and a system is identified. Apparently, at small radii, most systems are isolated single galaxies, the rest being close double and multiple galaxies. At larger radii, groups and clusters of galaxies and even superclusters will be formed. Superclusters are the largest nonpercolating galaxy systems that contain clusters and groups of galaxies with their surrounding galaxy filaments (Einasto et al. 2001, 2006, 2007a, 2007b). By selecting different neighborhood radii, we can probe the structures at different scales.

The mean density of galaxies is $\bar{\rho} = N/V$ (N is the number of galaxies contained in the volume V). The Poisson radius (radius of the sphere with unit population) is $R_0 = (3/4\pi\bar{\rho})^{1/3}$. To compare samples with different number den-

ties we express all distances in dimensionless radii $r = R/R_0$. Poisson radii (comoving distance) are 7.57 Mpc for the S1 sample, 6.44 Mpc for the S2 sample, and 5.35 Mpc for the S3 sample.

4. COLOR DEPENDENCE OF CLUSTERING PROPERTIES

In order to study how the geometry of the systems changes with increasing neighborhood radius, we calculate the maximum lengths of the systems. The maximal length of a system is defined as the maximum distance between members of this system. The largest system has the longest maximum length, but often it is not the richest system with the most member galaxies. Figure 1 shows the galaxy number N_{max} of the richest system and the maximal length D_{max} of the largest system as a function of the dimensionless radius r for three samples. As Deng et al. (2008) did, we define $L_0 = V^{1/3}$ (the edge length of the cube) as the rough estimate of the edge length of the sample volume V and express the maximal length of the largest system as dimensionless length $d_{\text{max}} = D_{\text{max}}/L_0$. The edge length L_0 is 329.68 Mpc for the three samples. Using three-dimensional cluster analysis, Deng et al. (2006) studied the super-large-scale structures in the flux-limited main galaxy sample and identified the CFA Great Wall (Geller & Huchra 1989) and the Sloan Great Wall (Gott et al. 2005) at dimensionless radii $r = 0.65$ and $r = 0.69$. The Sloan Great Wall is located at a median redshift of $z = 0.07804$, with a total length of about $433 h^{-1} \text{ Mpc}$ and a mean galaxy density about 6 times larger than that of the main galaxy sample. It is actually a well-known Abell supercluster SCL126 cataloged by Einasto et al. (2001) and also seen in the 2DF supercluster sample (Einasto et al. 2007a, 2007b). The size of the supercluster according to the Abell cluster and 2DF data is much smaller than that found by Deng et al.

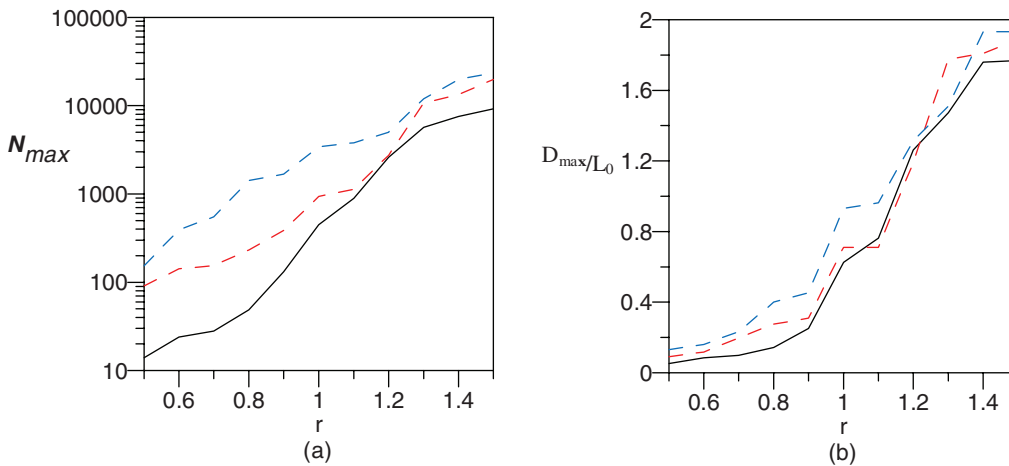


FIG. 1.—Clustering properties for the S1 (black line), S2 (red line), and S3 (blue line) samples: (a) the galaxy number N_{max} of the richest system; (b) the maximal length D_{max}/L_0 of the largest system, as a function of the dimensionless radius r .

(2006), mainly due to selection effects and difference in the use of the neighborhood radius to define superclusters. The CFA Great Wall is located at a median redshift of $z = 0.03058$, with a total length of about $251 h^{-1}$ Mpc (luminosity distance). But in our three samples with different $g-r$ color bins, such super-large-scale structures are not observed. For small radii ($r < 0.70$), the galaxy systems by cluster analysis consist mostly of isolated galaxies, as well as close double and multiple galaxies. A few systems form groups (in the S1 sample) and conventional clusters of galaxies (in the S2 and S3 samples). At dimensionless radius $r = 0.70$, the richest system only contains 28 galaxies in the S1 sample, 155 galaxies in the S2 sample, and 552 galaxies in the S3 sample; the maximal length of the largest system is 32.61 Mpc in the S1 sample, 65.35 Mpc in the S2 sample, and 77.14 Mpc in the S3 sample. These richest and largest systems actually are groups or clusters of galaxies. Even at dimensionless radius $r = 1.0$ (if the distribution of galaxies is uniform, all galaxies merge into a huge network at this radius), the richest system only contains 448 galaxies in the S1 sample, 938 galaxies in the S2 sample, and 3432 galaxies in the S3 sample; the maximal length of the largest system is 206.37 Mpc in the S1 sample, 234.59 Mpc in the S2 sample, and 307.16 Mpc in the S3 sample—all much smaller than the Sloan Great Wall. At radius $r = 1.1$, systems begin to merge into filamentary superclusters and finally into the entire interconnected supercluster network or the “cosmic web.” In a sample with larger number densities, richer and larger systems can be more easily formed. In Figure 1, we observe such a trend. Although many authors used dimensionless radii to express distances, we still suspect that this replacement cannot completely correct above bias. It is possible that the super-large-scale structures observed in the flux-limited main galaxy sample are partially due to this drawback of cluster analysis.

Figure 2 shows the average size of the systems (not including isolated galaxies) versus dimensionless radii for galaxy samples

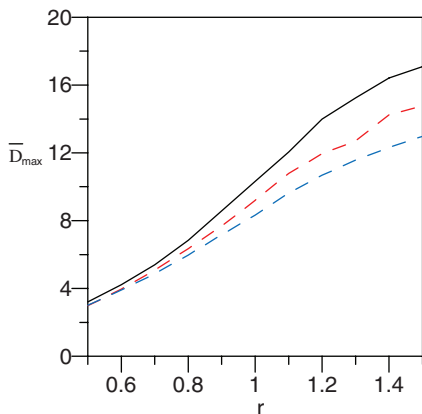


FIG. 2.—Average size of systems as a function of the dimensionless radius r for the S1 (black line), S2 (red line), and S3 (blue line) samples.

with different colors. We note that with an increase in the number densities of samples the average size of the systems preferentially become smaller. In fact, in a sample with a smaller number density, systems preferentially are larger than the ones with the same number of member galaxies in a sample with larger number densities.

With increasing neighborhood radius, various systems merge into strings and later into a string network. At a certain critical radius r_c , called the percolation radius, the largest string system reaches the opposite sidewalls of the sample. In this study, the percolation radius r_c is defined as the radius at which the maximal length D_{\max} of the largest system approximate to the edge length L_0 , with values $r_c \approx 1.19$ for the S1 sample, $r_c \approx 1.18$ for the S2 sample, and $r_c \approx 1.16$ for the S3 sample. As indicated by Einasto et al. (1984), the percolation radius depends on two factors: the degree of clustering and the degree of concentration of the strings. It is evident that the more filamentary the structure is, the easier it is to reach percolation. The percolation radius r_c is a good indicator of the filamentary structure. According to the studies of Pandey & Bharadwaj (2006, 2008), the blue galaxies have a more filamentary distribution than red galaxies. But in this study, we do not observe such a trend. The percolation radius r_c of our three samples with different $g-r$ color bins are nearly the same.

In order to describe the distribution of systems having different sizes, we analyze the multiplicity functions: the fraction of galaxies in systems of membership from n to $n + dn$ that depend on the dimensionless radii r . We divide the interval from 1 to N (the total number of galaxies) into 7 subintervals ($n = 1$, $2 \leq n < 5$, $5 \leq n < 20$, $20 \leq n < 50$, $50 \leq n < 100$, $100 \leq n < 200$, $n \geq 200$), and then construct histograms of the multiplicity functions at different radii ($r = 0.7$, $r = 0.8$, $r = 0.9$). In each histogram, systems that contain one galaxy are in the first bin, systems that contain from two to four galaxies are in the second bin, systems with five to nineteen galaxies in the third bin, and so on.

In Figure 3, the multiplicity functions are shown for three samples. The (1σ) error bars are Poissonian errors. As seen from this figure, the redder galaxies preferentially inhabit the dense groups and clusters. This is consistent with a widely accepted conclusion: luminous, red, and early-type galaxies exist preferentially in the densest regions of the universe. We also should note, however, that in our study the samples with the redder galaxies have larger number densities. As a result, richer and larger systems can be more easily formed in such samples.

When comparing samples with different number densities, we should explore the influence of the densities of samples on conclusions of cluster analysis, even if dimensionless radii are used to express distances. This is not a physical effect. Thus, across different color ranges, we also construct three samples with nearly the same number density, labeled SS1–SS3, and again perform the above analyses. SS1 contains 37,803 galaxies

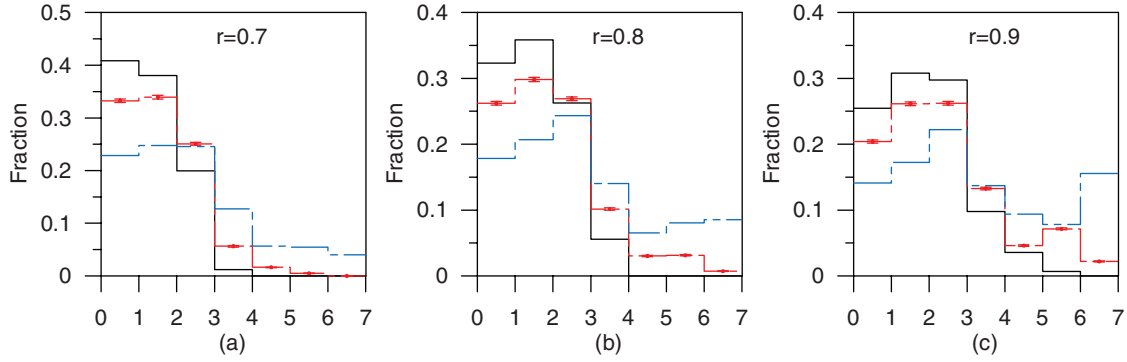


FIG. 3.—Histograms of multiplicity functions for the S1 (black line), S2 (red line), and S3 (blue line) samples at different radii: (a) at $r = 0.7$; (b) at $r = 0.8$; (c) at $r = 0.9$. The error bars for the S2 sample are 1σ Poissonian errors. Error bars for the S1 and S3 samples are omitted for clarity.

with the color range $g-r \leq 0.7$; SS2 includes 37,481 galaxies with the color range $0.7 \leq g-r < 0.865$; SS3 has 37,605 galaxies with the color range $g-r \geq 0.865$. Figure 4 shows the galaxy number N_{\max} of the richest system and the maximal length D_{\max} of the largest system as a function of the dimensionless radius r for the SS1, SS2, and SS3 samples. We still observe that richer and larger systems can be more easily formed in the redder samples. Figure 5 presents the average size of the systems (not including isolated galaxies) versus dimensionless radii for the SS1, SS2, and SS3 samples. As seen from this figure, among three different color samples with nearly the same number density, the difference in the average size of the systems as a function of the dimensionless radius r apparently becomes smaller. This correlation shows that when using cluster analysis we must be cautious about the differences of clustering properties produced by the different number densities of samples, even if dimensionless radii are used to express distances. In

addition, in Figure 5, we note that in the samples with redder color the average size of the systems as a function of the dimensionless radius r preferentially becomes larger. Like Figure 3, Figure 6 still shows that the redder galaxies preferentially inhabit the dense groups and clusters. These results confirm that the clustering properties of galaxies apparently depend on color.

The percolation radius r_c of three different color samples with nearly the same number density are $r_c \approx 1.21$ for the SS1 sample, $r_c \approx 1.22$ for the SS2 sample, and $r_c \approx 1.04$ for the SS3 sample. Such results seemingly show that the structure of the reddest sample is more filamentary, a finding that is not consistent with the conclusion obtained by Pandey & Bharadwaj (2006, 2008). We note that this conclusion is also different from the one obtained in the S1–S3 samples. This further shows that some conclusions or parameters of the cluster analysis depend on the densities of the galaxy samples, even if dimension-

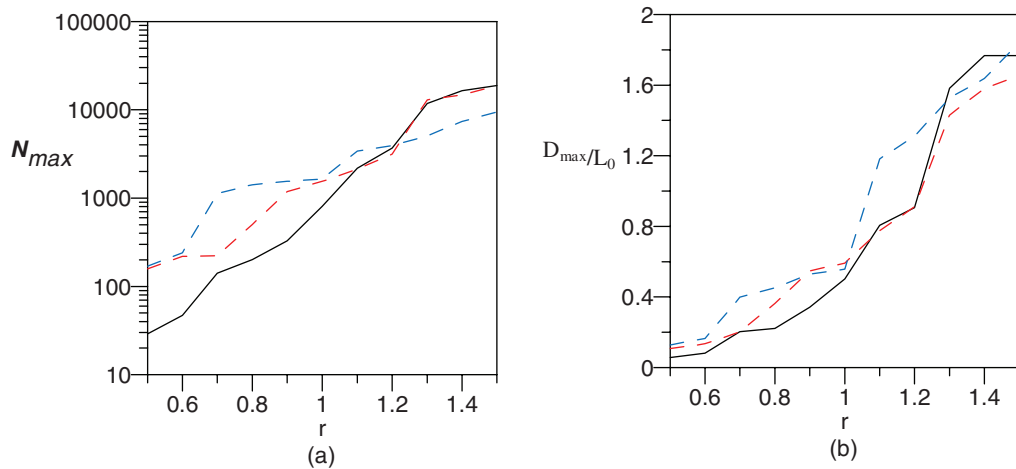


FIG. 4.—Clustering properties for the SS1 (black line), SS2 (red line), and SS3 (blue line) samples: (a) the galaxy number N_{\max} of the richest system; (b) the maximal length D_{\max}/L_0 of the largest system, as a function of the dimensionless radius r .

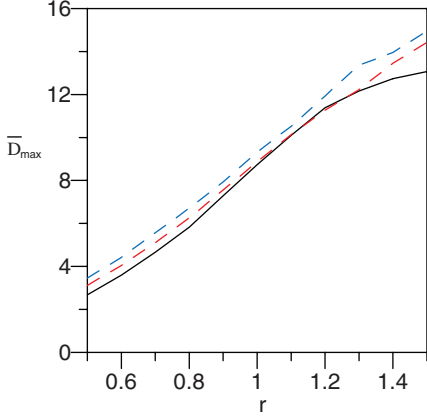


FIG. 5.—Average size of systems as a function of the dimensionless radius r for the SS1 (black line), SS2 (red line), and SS3 (blue line) samples

less radii are used for expressing all distances. To avoid this, we suggest that the simplest method is to construct samples with the same density. It is noteworthy that the percolation radius r_c is very sensitive to the selection of samples. If a sample contains a huge super-large-scale structure, different sampling means different divisions of this super-large-scale structure, which may result in different structure parameters of subsamples because any super-large-scale structure is fairly complicated. This is a limitation of the percolation radius of such studies. So, we believe that the percolation radius r_c is a good indicator only for the measure of the typical filamentary structure. In this study, at least, we have difficulty reaching any conclusions about the color dependence of the filaments based only on the percolation radius.

In order to further investigate the influence of the number densities of samples on clustering properties, we randomly extract from the S2 and S3 samples subsamples that have the same galaxy number and number density as the S1 sample,

respectively, and again perform the above analyses. We hope to use a different method for constructing samples with the same density and explore the difference of results between two methods. Figure 7 shows the galaxy number N_{\max} of the richest system and the maximal length of the largest system as a function of the dimensionless radius r for the S1, RS2 (the random subsample from S2), and RS3 (the random subsample from S3) samples. At dimensionless radii $r < 1.0$, we still observe that richer and larger systems can be more easily formed in the redder samples. The percolation radius r_c of three samples are $r_c \approx 1.19$ for the S1 sample, $r_c \approx 1.20$ for the RS2 sample, and $r_c \approx 1.20$ for the RS3 sample, which are still nearly the same. In Figures 8 and 9, we can reach the same conclusions as we did for the SS1–SS3 samples. This consistency shows that although some conclusions or parameters of the cluster analysis depend on the densities of the galaxy samples, a real physical effect is still observed: the redder galaxies preferentially inhabit the dense groups and clusters.

5. SUMMARY

In this study, we aim to investigate the color dependence of clustering properties. Like other authors (e.g., Blanton et al. 2005), we construct three galaxy samples with $g-r$ color bins of width 0.2, and fairly different number densities. When comparing samples with different number densities, the differences in the number densities of the samples may result in a difference of clustering properties among samples, even if dimensionless radii are used to express distances. This is not a physical effect. Thus, across different color ranges, we construct three samples with nearly the same number density. We also try another, different method for constructing samples with the same density, and randomly extract subsamples from the S2 and S3 samples, which have the same galaxy number and number density, respectively, as the S1 sample and perform the same analyses. Our conclusions follow:

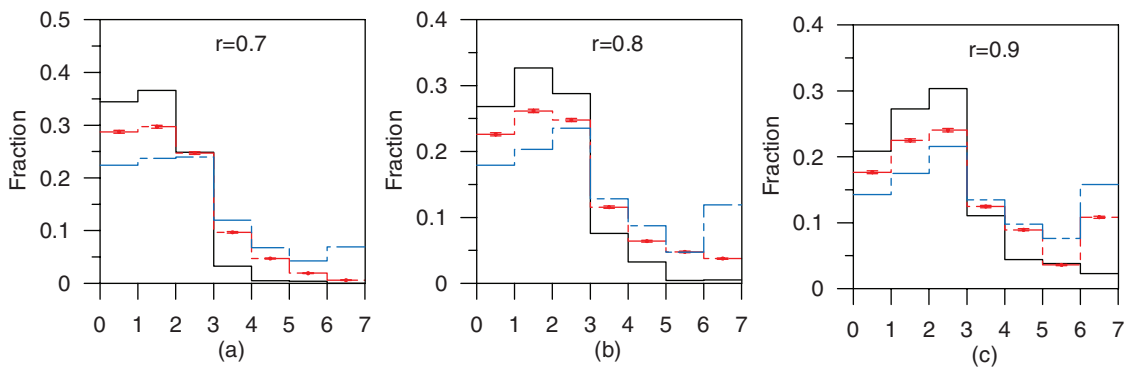


FIG. 6.—Histograms of multiplicity functions for the SS1 (black line), SS2 (red line), and SS3 (blue line) samples at different radii: (a) at $r = 0.7$; (b) at $r = 0.8$; (c) at $r = 0.9$. The error bars for the SS2 sample are 1σ Poissonian errors. Error bars for the SS1 and SS3 samples are omitted for clarity.

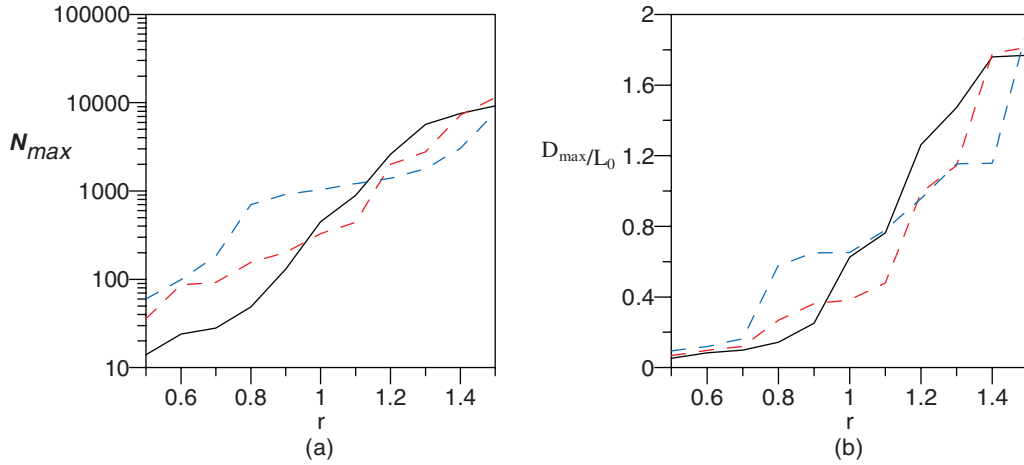


FIG. 7.—Clustering properties for the S1 (black line), RS2 (red line), and RS3 (blue line) samples: (a) the galaxy number N_{\max} of the richest system; (b) the maximal length D_{\max}/L_0 of the largest system, as a function of the dimensionless radius r .

1. In galaxy samples with different colors, super-large-scale structures are not observed, and richer and larger systems can be more easily formed in the redder samples. In addition, in the samples with redder color, the average size of the systems as a function of the dimensionless radius r preferentially become larger.

2. Because all analyses (including analyses in S1–S3, SS1–SS3, and S1–RS3) of the multiplicity functions reach the same conclusion, which actually shows that the conclusion about the multiplicity functions does not depend on the densities of the galaxy samples, we can then accept it without any caution: the redder galaxies preferentially inhabit the dense groups and clusters.

3. Based only on the percolation radius, we reach any conclusions about the color dependence of the filaments only with difficulty.

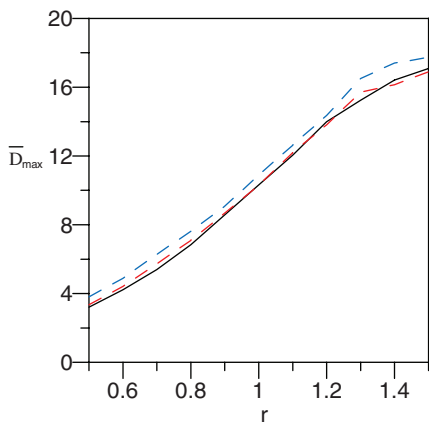


FIG. 8.—Average size of systems as a function of the dimensionless radius r for the S1 (black line), RS2 (red line), and RS3 (blue line) samples.

Finally, we should indicate that our analysis is not complete without a statistical test to test the color dependence of filamentarity, which requires analysis on multiple samples. In this study, it is very difficult to perform such a statistical test. Any method has its own limitations. The percolation radius r_c depends on many other factors, including sampling. Even at the key position of the sample, inserting or extracting a galaxy may result in a fairly large difference of the percolation thresholds. Actually, the percolation radius r_c only is a rough parameter. In this study, we use it and aim to see whether there are typical filamentary structures in our samples. In addition, we hope to investigate whether some conclusions or parameters of the cluster analysis depend on the densities of the galaxy samples.

We thank the anonymous referee for many useful comments and suggestions. Our study was supported by the National Natural Science Foundation of China (10863002) and also supported by the Program for Innovative Research Team of Nanchang University. Funding for the SDSS and SDSS-II has been provided by the Alfred P. Sloan Foundation, the Participating Institutions, the National Science Foundation, the US Department of Energy, the National Aeronautics and Space Administration, the Japanese Monbukagakusho, the Max Planck Society, and the Higher Education Funding Council for England. The SDSSWeb site is <http://www.sdss.org>. The SDSS is managed by the Astrophysical Research Consortium for the Participating Institutions. The Participating Institutions are the American Museum of Natural History, Astrophysical Institute Potsdam, University of Basel, University of Cambridge, Case Western Reserve University, University of Chicago, Drexel University, Fermilab, the Institute for Advanced Study, the Japan Participation Group, Johns Hopkins University, the Joint Institute for Nuclear Astrophysics, the Kavli Institute for Particle Astrophysics and Cosmology, the Korean Scientist Group, the Chinese Academy of Sciences

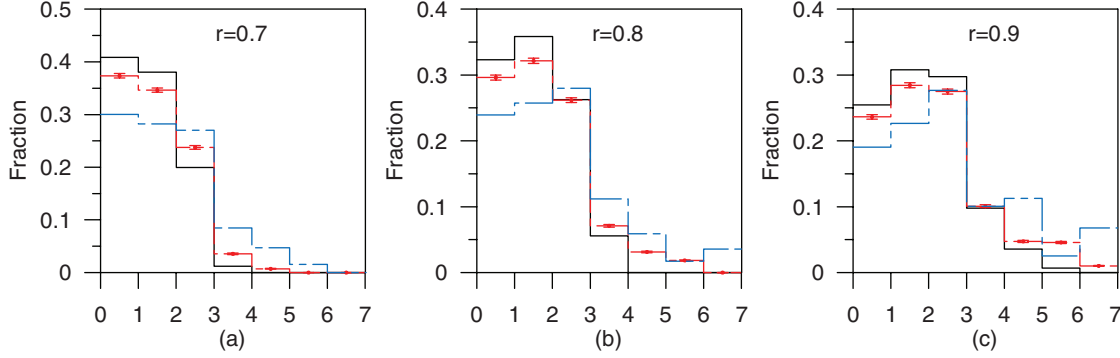


FIG. 9.—Histograms of multiplicity functions for the S1 (*black line*), RS2 (*red line*), and RS3 (*blue line*) samples at different radii: (a) at $r = 0.7$; (b) at $r = 0.8$; (c) at $r = 0.9$. The error bars for the RS2 sample are 1σ Poissonian errors. Error bars for the S1 and RS3 samples are omitted for clarity.

(LAMOST), Los Alamos National Laboratory, the Max Planck Institute for Astronomy (MPIA), the Max Planck Institute for Astrophysics (MPA), New Mexico State University, Ohio State

University, University of Pittsburgh, University of Portsmouth, Princeton University, the US Naval Observatory, and the University of Washington.

REFERENCES

- Adelman-McCarthy, J. K., Agüeros, M. A., & Allam, S. S., et al. 2008, *ApJS*, 175, 297
- Blanton, M. R., Eisenstein, D., & Hogg, D. W., et al. 2005, *ApJ*, 629, 143
- Brown, M. J. I., Webster, R. L., & Boyle, B. J. 2000, *MNRAS*, 317, 782
- Budavári, T., Connolly, A. J., & Szalay, A. S., et al. 2003, *ApJ*, 595, 59
- Carlberg, R. G., Yee, H. K. C., & Morris, S. L., et al. 2001, *ApJ*, 563, 736
- Davis, M., & Geller, M. J. 1976, *ApJ*, 208, 13
- Deng, X. F., Chen, Y. Q., & Zhang, Q., et al. 2006, *Chinese J. Astron. Astrophys.*, 6, 35
- Deng, X. F., He, J. Z., & Jiang, P. 2007, *ApJ*, 671, L101
- Deng, X. F., Zou, S. Y., & He, J. Z., et al. 2008, *Astron. Nachr.*, 329, 69
- Einasto, J., Einasto, M., & Saar, E., et al. 2006, *A&A*, 459, L1
- . 2007a, *A&A*, 462, 397
- Einasto, J., Einasto, M., & Tago, E., et al. 2007b, *A&A*, 462, 811
- Einasto, J., Klypin, A. A., & Saar, E., et al. 1984, *MNRAS* 206, 529
- Einasto, M., Einasto, J., & Tago, E., et al. 2001, *AJ*, 122, 2222
- Geller, M. J., & Huchra, J. P. 1989, *Science*, 246, 897
- Gott, J. R., Juric, M., & Schlegel, D., et al. 2005, *ApJ*, 624, 463
- Hogg, D. W., Blanton, M. R., & Eisenstein, D. J., et al. 2003, *ApJ*, 585, L5
- Loveday, J., Maddox, S. J., Efstathiou, G., & Peterson, B. A. 1995, *ApJ*, 442, 457
- Madgwick, D. S., Hawkins, E., & Lahav, O., et al. 2003, *MNRAS*, 344, 847
- Norberg, P., Baugh, C. M., & Hawkins, E., et al. 2001, *MNRAS*, 328, 64
- . 2002, *MNRAS*, 332, 827
- Park, C., Choi, Y. Y., & Vogeley, M. S., et al. 2005, *ApJ*, 633, 11
- Pandey, B., & Bharadwaj, S. 2006, *MNRAS*, 372, 827
- . 2007, *MNRAS*, 377, L15
- . 2008, *MNRAS*, 387, 767
- Stoughton, C., Lupton, R. H., & Bernardi, M., et al. 2002, *AJ*, 123, 485
- Strauss, M. A., Weinberg, D. H., & Lupton, R. H., et al. 2002, *AJ*, 124, 1810
- Zehavi, I., Blanton, M. R., & Frieman, J. A., et al. 2002, *ApJ*, 571, 172
- Zehavi, I., Zheng, Z., & Weinberg, D. H., et al. 2005, *ApJ*, 630, 1